

RESEARCH

Versatile Mobile Communications Simulation: The Vienna 5G Link Level Simulator

Stefan Pratschner^{1,2*}, Bashar Tahir^{1,2}, Ljiljana Marijanovic^{1,2}, Mariam Mussbah², Kiril Kirev², Ronald Nissel^{1,2}, Stefan Schwarz^{1,2} and Markus Rupp²

Abstract

Research and development of mobile communications systems require a detailed analysis and evaluation of novel technologies to further enhance spectral efficiency, connectivity and reliability. Due to the exponentially increasing demand of mobile broadband data rates and challenging requirements for latency and reliability, mobile communications specifications become increasingly complex to support ever more sophisticated techniques. For this reason, analytic analysis as well as measurement based investigations of link level methods soon encounter feasibility limitations. Therefore, computer aided numeric simulation is an important tool for investigation of wireless communications standards and is indispensable for analysis and developing future technologies. In this contribution, we introduce the Vienna 5G Link Level Simulator, a MATLAB-based link level simulation tool to facilitate research and development of 5G and beyond mobile communications. Our simulator enables standard compliant setups according to 4G Long Term Evolution, 5G new radio and even beyond, making it a very flexible simulation tool. Offered under an academic use license to fellow researchers it considerably enhances reproducibility in wireless communications research. We give a brief overview of our simulation platform and introduce unique features of our link level simulator in more detail to outline its versatile functionality.

Keywords: mobile communications; 5G; new radio; link level simulation

1 Introduction

Link level measurements, analysis and simulation are fundamental tools in the development of novel wireless communication systems, each offering its own unique benefits. Measurements provide the basis for channel modeling and are thus a prerequisite of analysis and simulations. Furthermore, measurement-based experiments present the ultimate performance benchmark of any transceiver architecture and are therefore indispensable in the system development cycle. However, performing measurements is very costly, time consuming and hard to adapt to specific communication scenarios; hence, their application is commonly kept at a necessary minimum. Compared to that, link level simulations facilitate rapid prototyping and comparison of competing technologies, enabling to gauge the potential of such technologies early on in the research and development process. A big advantage of analytic investigations is their potential to reveal pivotal relationships amongst key parameters of a sys-

tem; yet, analytic tractability often requires application of restrictive assumptions and simplifications, limiting the value of analytic results under realistic conditions. To investigate highly complex systems, such as wireless transceivers, and to efficiently evaluate the performance of novel technologies, link level simulations are thus often the preferred method of choice, enabling the incorporation of realistic and practical constraints/restrictions, which in many cases significantly alter the picture drawn by purely analytic investigations. Nevertheless, only by complementing measurements, analysis and simulations it is possible to reap the benefits of all three approaches.

In this paper, we present the newest member of our suite of Vienna Cellular Communications Simulators (VCCS): the Vienna 5G link level (LL) Simulator. Our mobile communications research group at the Institute of Telecommunications at TU Wien has a long and successful history of developing and sharing standard-compliant cellular communications simulators under an academic use license, with the goal of enhancing reproducibility in wireless communications academic research [1, 2]. The implementation of our work-horse

*Correspondence: spratsch@nt.tuwien.ac.at

¹Christian Doppler Laboratory for Dependable Wireless Connectivity for the Society in Motion

Full list of author information is available at the end of the article

of the past nine years, that is, the Vienna LTE Simulators [3], started back in 2009, leading to three reliable standard compliant LTE simulators: a downlink system level simulator [4, 5] and two link level simulators, one for uplink [6] and one for downlink [7]. Today the Vienna LTE Simulators count more than 50 000 downloads in total. Even though the path of 3rd Generation Partnership Project (3GPP) towards 5G is largely based on Long Term Evolution (LTE), we soon recognized that evolving our LTE simulators towards 5G is not straightforward due to a lack of flexibility of the simulation platform in terms of implementation and functionality. Mobile communications within 5G is expected to support much more heterogeneous and versatile use cases, such as enhanced mobile broadband (eMBB), massive machine-type communication (mMTC) or ultra-reliable and low-latency communication (uRLLC), as compared to 4G. Furthermore, a multitude of novel concepts and contender technologies within 5G, e.g., full-dimension/massive MIMO beamforming [8, 9, 10], mixed numerology multicarrier transmission [11, 12], non-orthogonal multiple access [13, 14], and transmission in the millimeter wave (mmWave) band [15, 16], requires careful identification, abstraction and modeling of key parameters that impact the performance of the system. We therefore decided to rather invest the required implementation effort into new simulators to extend our VCCS simulator suite and to evolve to the next generation of mobile communications with dedicated 5G link and system level simulators.

The Vienna 5G LL Simulator focuses on the physical layer (PHY) of the communication system. Correspondingly, the scope is on point-to-point simulations of the transmitter-receiver chain (channel coding, multiple-input multiple-output (MIMO) processing, multicarrier modulation, channel estimation, equalization,...) supporting a broad range of simulation parameters. Nevertheless, multi-point communications with a small number of transmitters and receivers are possible (limited only by computational complexity) to simulate, e.g., multi-point precoding techniques [17], rate splitting approaches [18], interference alignment concepts [19]. The transmission of signals over wireless channels thereby is implemented up to the individual signal samples and thus provides a very high level of detail and accuracy.

The Vienna 5G LL Simulator models the shared data channels of both, uplink and downlink transmissions, that is, the physical downlink shared channel (PDSCH) and the physical uplink shared channel (PUSCH). The simulator is implemented in MATLAB utilizing object oriented programming methods and its source code is available for download under an academic use license [2]; hence, we attempt to continue

our successful approach of facilitating reproducible research with this unifying simulation platform. The simulator allows for (and includes) parameter settings that lead to standard compliant systems, including LTE as well as 5G. Yet, the versatile functionality of the simulator provides the opportunity to go far beyond standard compliant simulations, enabling, e.g., the evaluation of a cornucopia of different combinations of PHY settings as well as the co-existence investigation of candidate 5G technologies. The Vienna 5G LL Simulator acts in close orchestration with its sibling the Vienna 5G system level (SL) Simulator: the LL simulator is employed to determine the PHY abstraction models utilized on SL to facilitate computationally efficient simulation of large-scale mobile networks.

2 Scientific Contribution

Computer aided numerical simulations are a well established tool for analysis and evaluation of wireless communications systems. Hence, a number of commercial and academic link level simulators is offered online. Amongst these tools, our new Vienna 5G LL Simulator supports a variety of unique features as well as a highly flexible implementation structure that allows for easy integration of additional components. In this section, we provide an overview of existing similar simulation platforms and compare them to our new simulator. We thereby restrict to academic tools that are, as our simulator, available for free, and leave aside commercial simulators. Further, we point out the distinct features offered by the Vienna 5G LL Simulator and thereby state our scientific contribution.

2.1 Related Work - Existing Simulation Tools

With each new wireless communications standard, the need for simulation emerges. This is necessary for the evaluation, comparison and further research as well as the development of communication schemes, specified within a certain standard. The existence of various simulation tools for the PHY of LTE, such as [20, 21] or the Vienna LTE-A LL Simulator [7, 6, 3], developed by our research group, supports this claim. These tools, however, are mainly based on 3GPP Release 8 to Release 10 and do not offer features and functionality specified and expected for 5G. There exist some commercial products, that is, link level simulators, that claim to support simulation of 5G scenarios. However, as we aim to support academic research also beyond the currently standardized features, we compare our Vienna 5G LL Simulator to other freely available academic simulators only. An overview of existing LL simulation tools is provided in Tab. 1.

The *GTEC 5G LL Simulator* is an open source link level simulator developed at the University of A

Table 1 Overview of existing LL simulators.

simulator \ property	language/platform	multi-link	waveforms	channel codes	flexible numerology
GTEC 5G LL Simulator	MATLAB	no	OFDM,FBMC	-	no
ns-3	C++, Python	yes	- (PHY model)	- (PHY model)	no
OpenAirInterface	C	yes	OFDM	turbo	no
Vienna 5G LL Simulator	MATLAB	yes	CP-OFDM,f-OFDM, FBMC,UFMC,WOLA	LDPC, turbo, polar, convolutional	yes

Coruña [22]. It is based on MATLAB and offers highly flexible implementation based on modules. By implementation of new modules, it is even possible to simulate different wireless communications standards, such as WiMAX or 5G. The current 5G module offers two PHY transmission waveforms, namely orthogonal frequency division multiplexing (OFDM) and filter-bank multicarrier (FBMC). Forward error correction channel coding is not supported. Further, this simulator focuses on single-link performance and does neither support multi-user nor multi-transmitter (multi base station (BS)) scenarios. Simulating inter-user interference (IUI) of non-orthogonal users, e.g., non-orthogonal multiple access (NOMA) or mixed numerology use-cases, is not possible with this tool.

A well known tool for simulation of communications networks is the *ns-3 simulator* [23], which is the successor of the *ns-2 simulator*. Although this tool has to be understood as a set of open source modules forming a generic network simulator, there exists an LTE module [24] that allows to simulate 4G networks. Further, there exists a module [25, 26] that covers mmWave propagation aspects of 5G. Still, the main focus of the *ns-3 simulator* lies on network simulations. The mentioned LTE module models radio resources with a granularity of resource blocks and does not consider time signals on a sample basis, as our simulator does. Therefore, the *ns-3 simulator* does not provide the detailed level of PHY accuracy that distinguishes pure link level simulation tools from system and network level simulators, where a certain degree of physical layer abstraction is unavoidable to manage computational complexity.

The *OpenAirInterface* is an open source platform offered by the Mobile Communications Department of EURECOM [27]. Currently the implementation is based on 3GPP Rel. 8 and supports only parts of later releases. The platform offers flexibility that allows for simulation of aspects of future mobile communications standards, such as cloud radio access network (RAN) or software defined networking. The simulation platform supports the simulation of the core network as well as the RAN and considers the complete protocol stack from the PHY to the network layer. It offers

two modes for PHY emulation, where the more detailed mode even considers actual transmission of signals over emulated channels. Still, this simulator focuses on simulation of networks in terms of a complete protocol stack implementation. However, details of PHY transmissions, such as waveform, channel coding, numerology or reference signals for channel estimation and synchronization, are not considered.

Accurate LL simulations require sophisticated channel models that realistically represent practically relevant propagation environments. Since 5G introduces novel PHY technologies, such as, full-dimension MIMO and transmission in the mmWave band, also channel models need to be updated and revised. The modular implementation structure of our simulator supports easy integration of dedicated wireless channel models and emulators, such as [28] or [29, 30].

2.2 Scientific Contribution and Novelty of our Simulator

The currently ongoing evolution from LTE towards 5G shows that LL simulations are still a very active research topic, since many different candidate RAN and PHY schemes need to be gauged and compared against each other. The Vienna 5G LL Simulator supports these needs and allows for a future-proof evaluation of PHY technologies due to its versatility. The simulator allows almost all PHY parameters to be chosen freely, such that any multi-carrier system can be simulated; specifically, by setting parameters according to standard specifications, it is possible to conduct standard-compliant simulation of LTE or 5G (we provide corresponding parameter files in the simulator package). Due to the modular structure and application of object oriented programming, further functionality, such as additional channel models, can easily be included.

Our LL simulator focuses on simulating PHY effects in a high level of detail. It considers the actual transmission of time signals over emulated wireless channels in a granularity of individual samples. This allows the detailed analysis of PHY schemes of current and future mobile communications systems, e.g., investigating the impact of the channel delay and Doppler spread on various PHY waveforms and numerologies (see Section 4.6).

The following specific aspects distinguish our Vienna 5G LL Simulator from the tools summarized in Section 2.1.

- *PHY methods even beyond 5G*: As mentioned above, the simulator supports standard-compliant simulation of the PDSCH/PUSCH of LTE and 5G by implementing the signal processing chains described in [31, 32]. Yet, simulation parameters of adaptive modulation and coding (AMC), MIMO processing and baseband multicarrier waveforms are not restricted to standard-compliant values. In addition, the modular simulator structure allows for easy integration of novel functionality, such as additional waveforms or modulation and coding schemes (MCSs), to investigate candidate technologies of future mobile communication systems. As an example, we have implemented FBMC transmission to support comparison with the filtered/windowed OFDM-based waveforms considered within 5G standardizations (weighted overlap and add (WOLA), universal filtered multicarrier (UFMC), filtered OFDM (f-OFDM)).
- *Flexible numerology*: As introduced by 3GPP for 5G, the concept of flexible numerology describes the possibility to adapt the time and frequency span of a resource element. This means, that the subcarrier spacing and the symbol duration of the multicarrier waveform are adaptable to support a variety of service requirements (latency, coverage, throughput), channel conditions (delay or Doppler spread) and carrier frequencies. As these parameters are freely adjustable in our simulator, effects of different numerologies are investigatable, even beyond the standardized range [32]. To summarize, the simulator enables comparison and optimization of numerologies of several multicarrier waveforms (see Section 4.2) in combination with various channel codes (see Section 4.1) under arbitrary channel conditions in terms of delay and Doppler spread.
- *Multi-link simulations*: The Vienna 5G LL Simulator is capable of simulating multiple users and BSs (only restricted by computational complexity). Although analysis of large networks with a high number of users and BSs is not the goal of a link level simulation, this feature allows investigation of IUI. While this feature was not required for LTE's LL, since user signals within a cell were automatically orthogonal due to the application of OFDM with a fixed numerology, it is interesting in the context of 5G as users with different numerologies are not orthogonal anymore. The Vienna 5G LL Simulator enables the investigation of IUI in such mixed numerology use-cases.

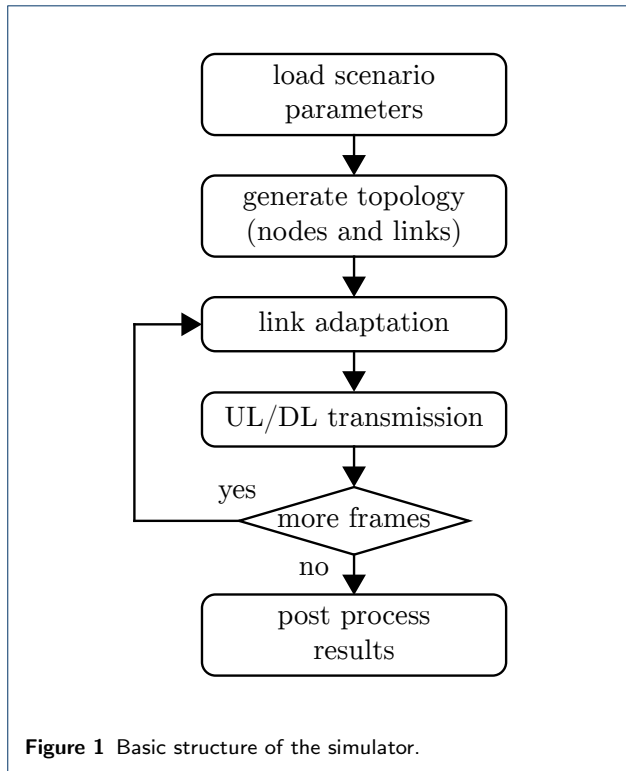
3 Simulator Structure

In this section we provide a short general description of the Vienna 5G LL Simulator and a brief introduction of the simulator's structure. In addition to this overview, supplementary documents, such as a user manual as well as a detailed list of features, are provided on our dedicated simulator web page [2].

Link level simulations in most cases assume a fixed signal-to-noise ratio (SNR) for the transmission link between transmitter and receiver. We slightly deviate from this common approach in our simulator, since we support multiple different waveforms that achieve different SNRs for a given total transmit power. Hence, rather than fixing the SNR, we fix the transmit and noise power and determine the SNR as a function of the applied waveform. Additionally, since we support multi-link transmissions, we introduce individual path loss parameters for these links, to enable controlling the SIR of the individual connections. However, in contrast to a SL simulator, we do not introduce a spatial network geometry to determine the path loss, but rather set the path loss as an input parameter of the simulator. The goal of LL simulations is to obtain results in terms of PHY performance metrics, such as throughput, bit error ratio (BER) or frame error ratio (FER), which are representative for the average system performance within the specified scenario. To this end, Monte Carlo simulations are carried out and results are averaged over a certain number of channel, noise and data realizations. To gauge the statistical significance of the obtained results, the simulator calculates the corresponding 95 percentile confidence intervals.

Fig. 1 illustrates the basic processing and simulation steps applied by the simulator. The initial step is to specify and supply a scenario file to the simulator. The file contains all the information necessary for the simulation. Setting up a scenario begins with the specification of the network topology, that is, defining all the nodes and their associated connections in the network. The nodes take the role of either a BS or a user. Arbitrarily meshed connections between these nodes are supported. The connections can serve as downlink, uplink, or sidelink (device-to-device link). Furthermore, inter- and intra-cell interference is easily captured, as it only requires to establish the corresponding connections between the supposedly interfering nodes.

Every connection is represented in the simulator by a so-called link object. It is the most fundamental building block of the simulator and contains all the PHY functionality objects, such as, channel coding, modulation, MIMO processing, channel generation and estimation, channel state information (CSI) feedback calculation, etc. Moreover, the link object also contains the generated signals throughout the whole transceiver chain of the specific connection.



After the network topology is specified, the next step in the scenario setup is to enter the transmission parameters. This covers the whole transmission chain, including the specification of the applied channel coding scheme, the multicarrier waveform, the applied channel model, as well as the equalizers and decoders employed by the receiver. Parameters can either be set locally for each link and node, or conveniently globally, in case all links and nodes use the same settings. Setting different parameters for different links enables coexistence investigations of multiple technologies; for example, one cell could be set up to operate with OFDM and turbo coding while the other cell uses FBMC with low-density parity-check (LDPC) coding. This allows to investigate the sensitivity w.r.t. out-of-cell interference of such systems. Notice, since signals are processed on a sample basis, the modeling of such interference is highly accurate.

Once the scenario file is ready, it gets loaded by the main script of the simulator, where the simulation is set up according to the input topology and parameters. The simulation is carried out on a frame-by-frame basis over a specified sweep parameter, such as the path loss, transmit power, or velocity^[1]. Within the simula-

^[1]Please note, that the velocity determines the maximum Doppler shift of the user's channel. As there is no geometry in an LL simulator, the user has no physical position that changes over time.

tion, the simulator performs full down- and uplink operation of all specified transmission links, including the possibility to activate LTE compliant CSI feedback as well as link adaptation in terms of AMC and standard-compliant MIMO processing (see Section 4.4). The results for all nodes in the form of throughput, FER, and BER versus the sweep parameter (e.g., SNR) are provided as simulator output. In addition to these aggregated results, the simulator also stores simulation results of individual frames, to support further post-processing by the researcher. The overall procedure is optimized in such a way that the overhead of the exchanged information during the simulation is minimal, and the operations are executed efficiently. Moreover, parallelism can be enabled over the loop of the sweep parameter, which offers a substantial reduction in simulation time when run on multi-processor machines.

4 Features

In this section, we provide a more detailed description of the Vienna 5G LL Simulator. The main components and features are described, giving insights in the available versatile functionality. To highlight features, that make our LL simulator unique, we further provide and discuss results of exemplary simulations. All of these example scenarios are included with the simulator download package and are straightforward to reproduce.

4.1 Channel Coding

The first processing block in the transmission chain is channel coding, where error correction and detection capability is provided to the transmitted signal. The simulator supports the four coding schemes of convolutional, turbo, LDPC, and polar codes. These schemes were selected by 3GPP as the candidates for 5G, due to their excellent performance and low complexity state-of-the-art implementation. Tab. 2 summarizes the supported channel coding schemes and their corresponding decoding algorithms.

The turbo and convolutional codes are based on the LTE [33] standard, the LDPC code follows the 5G new radio (NR) [34] specifications, and for polar codes we currently use the custom construction in [35] concatenated with an outer cyclic redundancy check (CRC) code. This includes both the construction of the codes and also the whole segmentation and rate matching process as defined in the standards.

The decoding of convolutional and turbo codes is based on the log-domain BCJR algorithm [36], that is, the Log-MAP algorithm, and its low complexity variants of MAX-Log-MAP [37] and Linear-Log-MAP [38]. For the LDPC code, the decoder employs the Sum-Product algorithm [39], and its approximations of the

Table 2 Supported channel coding schemes.

scheme	construction/ encoding	decoding algorithms
turbo	LTE	Log-MAP Linear-Log-MAP MAX-Log-MAP
LDPC	5G NR	Sum-Product PWL-Min-Sum Min-Sum
polar	currently custom	SC List-SC CRC-List-SC
convolutional	LTE	Log-MAP MAX-Log-MAP

Min-Sum [40] as well as the double piecewise linear PWL-Min-Sum [41]. The LDPC decoder utilizes a layered architecture where the column message passing schedule in [42] is applied. This allows for faster convergence in terms of the decoding iterations. As for polar codes, the decoder is based on the log-domain successive cancellation (SC) [43], and its extensions of List-SC and CRC-aided List-SC [44].

In the remainder of this section, we consider an example simulation on channel coding performance with short block length. The study of channel codes for short block lengths in combination with low code rates, is of interest in many applications. Typical examples are the control channels of cellular systems, and the 5G mMTC and uRLLC scenarios. Here, we investigate the aspects of such combination using convolutional, turbo, LDPC, and polar codes. In order to do that, we need to have a complete freedom in setting the parameters of the block length and code rate. Thanks to the modular structure of the simulator, we can use the channel coding object in a standalone fashion, thus eliminating the restrictions imposed by the other parts of the transmission chain, such as the number of scheduled resources or the target code rate for given channel conditions. Tab. 3 lists the simulation parameters of our setup. For the decoding iterations and list size, we employ relatively large values to maximize the performance of the decoding algorithm.

For the LDPC code, filler bits were added to the input block. This is necessary to compensate the mismatch between the chosen block length and the dimensions of the 5G NR parity check matrix. However, the addition of filler bits reduces the effective code rate, since it results in a longer output codeword. For this reason, we further puncture the output in such a way that the target length and code rate are met. This might have a negative impact on the performance of the LDPC code, as some parts of the codeword belong to the extra filler bits which are discarded after

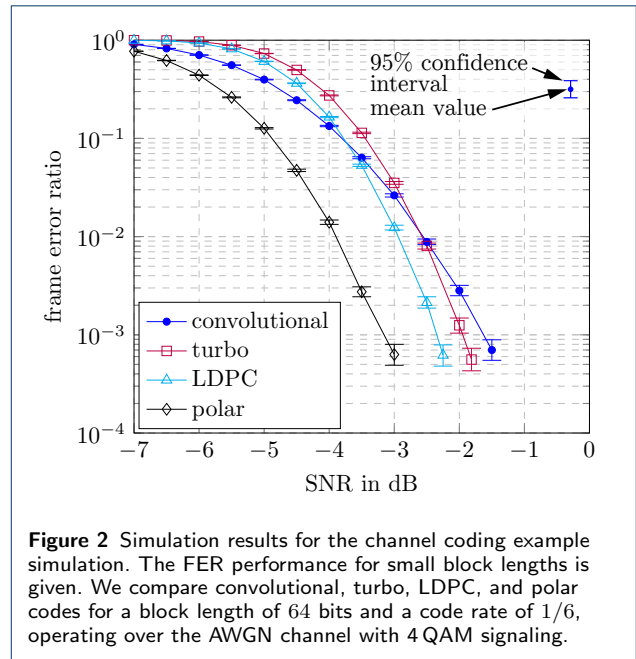


Figure 2 Simulation results for the channel coding example simulation. The FER performance for small block lengths is given. We compare convolutional, turbo, LDPC, and polar codes for a block length of 64 bits and a code rate of 1/6, operating over the AWGN channel with 4 QAM signaling.

decoding. Nonetheless, by following this procedure we guarantee that all the schemes are running with the same code rate.

Fig. 2 shows the FER performance of the aforementioned coding schemes. It can be seen that the polar code has the best performance in such setup. Namely, at the FER of 10^{-2} , the polar code is leading by 1 dB against the LDPC code, and by 1.5 dB against the turbo and convolutional codes. At the lower regime of the FER, the gap appears to get narrower. Still, the polar code remains the clear winner. This makes it an attractive choice for the scenarios of short block length. However, other factors which are not considered here, such as decoding latency or hardware implementation aspects, influence the choice of a coding scheme.

4.2 Modulation

According to the current 3GPP specifications related to the NR PHY design, equipment manufacturers are unconstrained in the choice of OFDM-based multicarrier waveforms [45]. Cyclic prefix OFDM (CP-OFDM) will be the baseline multicarrier transmission scheme applied in 5G. However, to reduce out of band (OOB) emissions and improve spectral confinement, manufacturers are free to add windowing or filtering on top of CP-OFDM. Our simulator offers the versatility to support various multicarrier waveforms. Besides OFDM-based waveforms, such as, CP-OFDM, WOLA, UFMC, f-OFDM, we additionally support FBMC as a promising candidate for the next generations beyond 5G [46]. In the following we provide a brief description of each waveform supported by our simulator. The

Table 3 The simulation parameters of the channel coding for short block lengths example. Three different channel codes are compared for the same short block length.

parameter	value			
channel code	convolutional	turbo	LDPC	polar
decoder	MAX-Log-MAP	Linear-Log-MAP	PWL-Min-Sum	CRC-List-SC
iterations/list size	-	16	32	32
block length	64 bits (48 info + 16 CRC)			
code rate	1/6			
modulation	4 QAM			
channel	AWGN			

basic signal flowcharts applied for signal generation and reception at the transmitter and receiver, respectively, for all of these waveforms are shown in Figs. 3 and 4. In general, the filtering and windowing operations are applied in time domain, after the inverse fast Fourier transform (IFFT). Depending on the modulation scheme, these operations are performed per subband (UFMC), per subcarrier (WOLA,FBMC) or on the whole band (f-OFDM). Some of the schemes employ cyclic prefix (CP), such as CP-OFDM, WOLA and f-OFDM, or zero prefix (ZP), such as UFMC, in order to prevent distortion caused by the multipath channel and by filtering or windowing. To mitigate potential IUI (or inter-subband interference), windowing/filtering is also applied at the receiver side [47].

4.2.1 Cyclic Prefix OFDM

Proposed in the downlink of the current LTE system, CP-OFDM is currently the most prominent multicarrier waveform, since it is the standardized waveform not only of LTE downlink, but also for WiFi 802.11 [48]. It assumes a rectangular pulse of duration $T = T_{\text{OFDM}} + T_{\text{CP}}$ at the transmitter, where T_{OFDM} is the useful symbol duration and T_{CP} is the length of CP. This pulse shape enables very efficient implementation by means of an IFFT at the transmitter side and an FFT at the receiver side. Unfortunately, the rectangular pulse also causes high OOB emissions. By applying a CP the scheme avoids intersymbol interference (ISI) and preserves orthogonality between subcarriers in the case of highly frequency selective channels. This simplifies equalization in frequency-selective channels, enabling the use of simple one-tap equalizers, but reduces the spectral efficiency at the same time due to the CP overhead.

4.2.2 Weighted Overlap and Add

WOLA extends OFDM by applying signal windowing in the time domain [49]. Unlike conventional OFDM, which employs a rectangular prototype pulse, WOLA applies a window that smooths the edges of the rectangular pulse, improving spectrum utilization. The window shape is based on the (root) raised cosine function

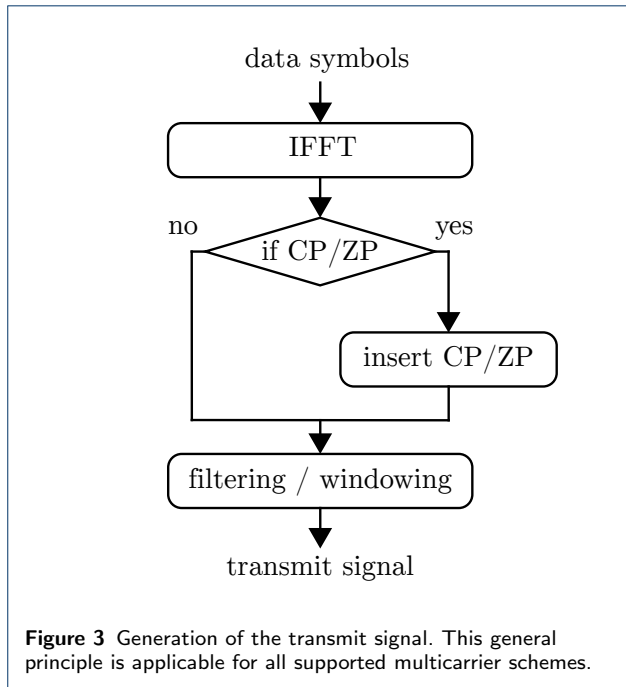
determined by a roll-off factor that controls the windowing function. Due to this windowing function, consecutive WOLA symbols overlap in time. This effect is compensated for by extending the length of the CP. In that way the scheme preserves the orthogonality of symbols and subcarriers, but it increases the overhead of the CP and therefore reduces the spectral efficiency compared to OFDM. At the receiver side, windowing in combination with an overlap and add operation further reduces IUI [46].

4.2.3 Universal Filtered Multicarrier

As an alternative to windowing, filtering can be applied to OFDM waveforms to reduce out-of-band emissions. UFMC employs subband-wise filtering of OFDM and is therefore an applicable waveform for 5G NR [50]. Compared to OFDM, UFMC provides better suppression of side lobes and supports more efficient utilization of fragmented spectrum. In our simulator, we follow the transceiver structure proposed in [51, 50]. At the transmitter side we apply a subband-wise IFFT, generating the transmit signal in time domain. In order to reduce OOB emissions we apply filtering on a set of contiguous subcarriers, so called subbands. There are several criteria for the filter design. In our simulator, we employ the Dolph-Chebyshev filter since it maximizes the side lobe attenuation [52]; however, other filters can easily be implemented. UFMC employs a ZP in order to avoid ISI on time dispersive channels, although there are only minor differences compared to the utilization of a CP [53]. To restore the cyclic convolution property similar to CP-OFDM, which enables low-complexity FFT-based equalization, the tail of the received signal is added to its beginning at the receiver side.

4.2.4 Filtered OFDM

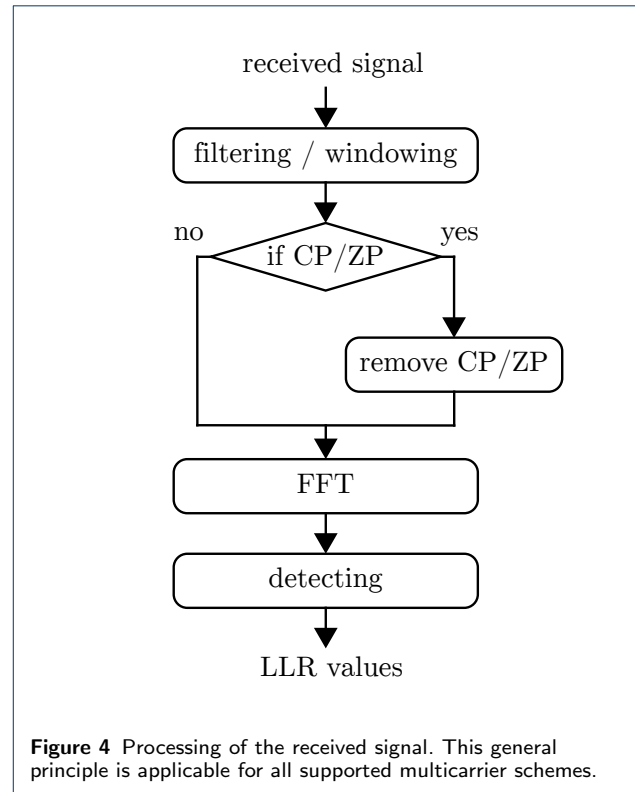
Very similar to UFMC is f-OFDM; however, unlike UFMC, which applies filtering on a chunk of consecutive subcarriers, f-OFDM includes a much larger number of subcarriers which are generally associated to different use cases [54]. f-OFDM employs filtering at both, transmitter and receiver side. If the total



CP length is longer than the combined filter lengths, the scheme restores orthogonality in an additive white Gaussian noise (AWGN) channel. Hence, compared to CP-OFDM, the CP length is generally longer and thus the overhead is increased. However, in order to keep the overhead at a minimum, the method usually allows a small amount of self-interference. The introduced interference is controlled by the filter length and the CP length. Currently our simulator supports a filter based on a sinc pulse which is multiplied by a Hanning window, yet any other filter can easily be incorporated.

4.2.5 Filter-Bank Multicarrier

Although 3GPP decided that FBMC will not be employed in 5G, it still has many advantages compared to OFDM and is thus a viable candidate for the next generations beyond 5G. One of the most significant advantage is the low OOB emission. However, narrow subcarrier filters in the frequency domain imply overlapping of symbols in the time domain. FBMC does not achieve complex-valued orthogonality, but only orthogonality of real-valued signals. Nevertheless, in combination with offset-QAM, the same spectral efficiency as in OFDM can be achieved. Additionally, in the case of doubly-selective channels, the method is able to significantly suppress ISI and intercarrier interference (ICI) using conventional equalizers, such as a minimum mean squared error (MMSE) equalizer [55, 56]. However, for channel estimation or in the case of MIMO transmissions, imaginary interference has a more significant impact and requires a special treatment [57].

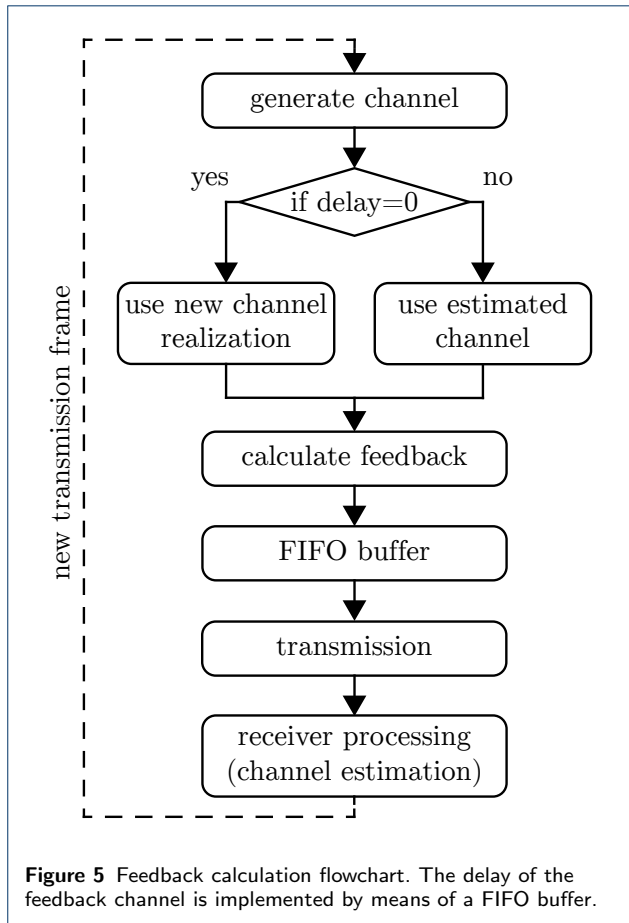


4.3 MIMO Transmissions

The Vienna 5G LL Simulator supports arbitrary antenna configurations and various MIMO transmission modes. Not only may the number of transmit and receive antennas be set to any value, also this parameter is individually adjustable for each node. The behavior of the MIMO transmitter and receiver is selected via the transmission mode. Currently the available options are transmit diversity, open loop spatial multiplexing (OLSM), closed loop spatial multiplexing (CLSM) and a custom transmission mode that is freely configurable. The transmit diversity mode leads to a standardized version of Alamouti's space-time codes [31]. OLSM and CLSM both are LTE standard compliant MIMO transmission modes, where link adaptation is performed according to Section 4.4. The additional custom transmission mode allows a flexible setting of parameters. For this configuration, the number of active spatial streams, the precoding matrix as well as the MIMO receiver are freely selectable. Currently zero forcing, MMSE, sphere decoding and maximum likelihood (ML) MIMO detectors are implemented.

4.4 Feedback

To adapt the transmission parameters to the current channel conditions, CSI at the transmitter is required. Since up- and downlink are implemented for frequency-division duplexing mode, the reciprocity of the channel



cannot be exploited. For non-reciprocal channels, the receiver has to estimate the channel and then feed back the CSI to the transmitter. To reduce the overhead, the fed back CSI is quantized. The feedback calculation is an intelligent way of quantizing the CSI, it comprises the precoding matrix indicator (PMI), rank indicator (RI) and channel quality indicator (CQI). By the CQI feedback the transmitter selects one of 15 MCSs. By the PMI the transmitter selects a precoding matrix from a codebook and the RI informs the transmitter about the number of active transmission layers.

The algorithm for calculation of the feedback parameters is based on [58, 59]. To reduce the complexity, the feedback calculation is decomposed into two separate steps. In the first step the optimum PMI and RI are jointly evaluated, maximizing the sum mutual information over all scheduled subcarriers. In the second step we choose the CQI with the largest rate that achieves a block error ratio below a certain threshold. The CQI value is found by mapping the post equalization signal to interference and noise ratio (SINR) of all scheduled subcarriers to an equivalent AWGN channel SNR.

Fig. 5 shows a flowchart describing the feedback process. The feedback channel is modeled as simple delay, which is implemented by means of a FIFO buffer of corresponding size; hence, we do not consider transmission errors in the feedback path, only the processing delay. For a feedback delay of $n > 0$, the estimated channel is used at the receiver for the feedback calculation. The calculated feedback is then fed into the FIFO buffer. For the first n transmissions, all three feedback parameters are set to the default value 1. The delay has to be sufficiently smaller than the coherence time to ensure similar channel conditions. The feedback calculation is placed after the generation of the channel and before the transmission. This enables simulations with instantaneous (zero delay) feedback as the newly generated channel is immediately available for the feedback calculation.

For the CLSM and OLSM transmission modes, the feedback is configured automatically, whereas for the custom transmission mode the feedback is configured manually in the scenario file. For all three transmission modes, the feedback delay and the type of averaging within the SINR mapping have to be set in the scenario file.

4.5 Channel Models

As the aim of LL simulation is acquisition of the average link performance, many random channel realizations are necessary per scenario. There exists no network geometry and therefore no path-loss model. A link's path-loss is an input parameter, determining the user's average SINR. Therefore, the channel model only includes small scale fading effects while its average power is dictated by the given path-loss.

The use of a universal spatial channel model, such as the QUADRIGA model [28] or the 3GPP 3D channel model [60, 61], is of limited benefit due to the lack of geometry. We offer frequency selective and time selective fading channel models. The frequency selectivity is implemented as tapped delay line (TDL) model. Currently we offer implementations for to Pedestrian A, Pedestrian B, Vehicular A [62], TDL-A to TDL-C [63], Extended Pedestrian A and Extended Vehicular A [64]. To model the channel's time selectivity, the fading taps change over time to fit a certain Doppler spectrum. A Jake's as well as an uniform Doppler spectrum are currently implemented. Jake's model also supports time-correlated fading across frames according to a model from [65] with a modification from the appendix of [66]. For time-invariant channels, the two-wave with diffuse power (TWDP) fading model [67] is employed, which is a generalization of the Rayleigh and Rician fading models. In contrast to the Rayleigh fading model, where only diffuse components are consid-

ered, and the Rician fading model, where a single specular component is added, two specular components together with multiple diffuse components are considered in the TWDP fading model. The two key parameters for this model are K and Δ . Similar to the Rician fading model, the parameter K represents the power ratio between the specular and diffuse components. The parameter Δ is related to the ratio between peak and average specular power and thus describes the power relationship between the two specular components. By proper choice of K and Δ , the TWDP fading model is able to characterize small scale fading for a wide range of propagation conditions, from no fading to hyper-Rayleigh fading. Tab. 4 shows typical parameter combinations and their corresponding fading statistic. In contrast to classical models, the TWDP fading model allows for destructive interference between two dominant specular components. This enables for a possible worse than Rayleigh fading behavior, depending on the fading model parameters.

Spatial correlation of MIMO channels is implemented via a Kronecker correlation model with correlation matrices as described in [68].

Table 4 Parameters of the TWDP fading model. For the case of a time-invariant channel, the TWDP fading is parametrized by K and Δ .

fading statistic	K	Δ
no fading	∞	0
Rician	> 0	0
Rayleigh	0	-
Hyper-Rayleigh	∞	≈ 1

4.6 Flexible Numerology

In this section, an example simulation scenario, demonstrating the concept of flexible numerology, is presented. As previously emphasized, one of the key advantages of our simulator compared to other simulators is the support of flexible numerology. According to 3GPP, there are three 5G use case families: uRLLC, mMTC and eMBB. In order to meet different requirements of a specific use case, 3GPP proposes a flexible PHY design in terms of numerology. Flexible numerology refers to the parametrization of the multicarrier scheme. It means that we are flexible to choose different subcarrier spacing and thus symbol and CP duration according to the desired latency, coverage or carrier frequency. On the other hand, the right choice of subcarrier spacing has to depend also on the channel conditions. We investigate the impact of different channel conditions for different numerologies in [69]. Additionally, in [69] we apply the optimal pilot pattern obtained accounting not only for the channel conditions, but also for the channel estimation error as a

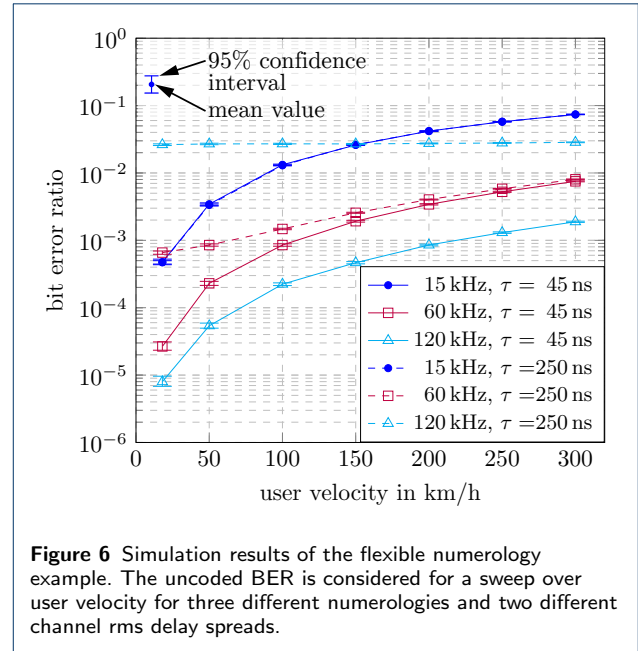


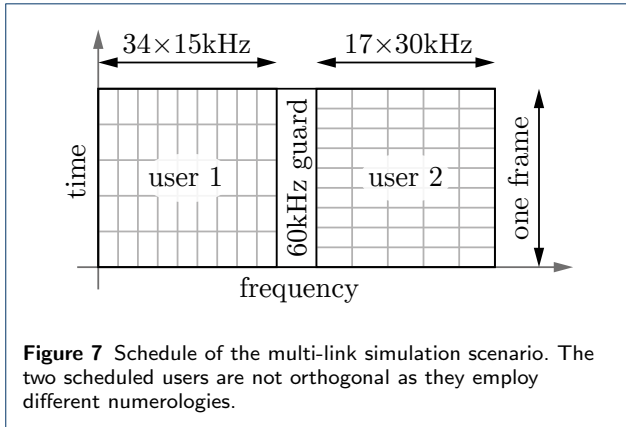
Figure 6 Simulation results of the flexible numerology example. The uncoded BER is considered for a sweep over user velocity for three different numerologies and two different channel rms delay spreads.

consequence of imperfect channel knowledge. In this section we assume perfect channel knowledge and investigate the sensitivity of different numerologies w.r.t. the delay and Doppler spread of the channel.

Table 5 Parameters for the flexible numerology simulation example. Three different numerologies are employed.

parameter	value		
subcarrier spacing	15 kHz	60 kHz	120 kHz
number of symbols per frame	14	56	112
CP duration	4.76 μ s	1.18 μ s	0.59 μ s
bandwidth	5.76 MHz		
carrier frequency	5.9 GHz		
modulation alphabet	64 QAM		
channel model	TDL-A		

The parameters used for the simulations shown in Fig. 6 are given in Tab. 5. According to 3GPP, subcarrier spacings for 5G are scaled versions of the basic 15 kHz subcarrier spacing by a factor 2^k , where k is an integer, in the range from 0 up to 5 [32]. In this simulation example we take three values for subcarrier spacings - 15 kHz, 60 kHz and 120 kHz. We keep the same bandwidth of 5.76 MHz using different subcarrier spacings, and vary the number of subcarriers and symbols proportionally. We employ the TDL-A channel model with two different root mean squared (rms) delay spreads of $\tau = 45$ ns and $\tau = 250$ ns [63]. The channel's time selectivity is determined according to Jake's Doppler spectrum where the maximum Doppler frequency is given by the user's velocity. In Fig. 6 we show the behavior of the BER versus user velocity, using the



5.9 GHz carrier frequency, which is typical for the vehicular communication scenarios. We want to show the impact of the Doppler shift and different channel delay spread on the different subcarrier spacings. In general, we observe that the BER increases with user velocity due to growing ICI. In case of the short rms delay spread, the transmission achieves a lower BER compared to larger subcarrier spacings, since the large subcarrier spacing is more robust to ICI and also the CP length is sufficient compared to the maximum channel delay spread. On the other hand, with the long rms delay spread channels, ISI is present with large subcarrier spacings due to insufficient CP length. In Fig. 6 ISI is already pronounced with 60 kHz. For 120 kHz, ISI dominates over ICI for the entire range of considered user velocities; hence, the BER curve is flat.

4.7 Multi-link Simulations

To demonstrate the capability of simulations employing multiple communication links of our simulator, we show a further example simulation in this section. Different users were inherently orthogonal due to the deployment of OFDM in LTE. Due to the concept of mixed numerologies in 5G or the employment of non-orthogonal waveforms in future mobile communications systems, users are not necessarily orthogonal anymore. As our simulator allows multiple communication links, it enables investigation of scenarios where users interfere with each other.

To demonstrate this feature, we consider an up-link transmission of two users with mixed numerology. User 1 employs a subcarrier spacing of 15 kHz while User 2 employs 30 kHz which makes them non-orthogonal. The users are scheduled next to each other in frequency as shown in Fig. 7. The guard band of 60 kHz is intended to reduce the IUI at the price of spectral efficiency. We consider User 1 as the primary user that suffers from interference generated by User 2. The BS's receiver is not interference aware.

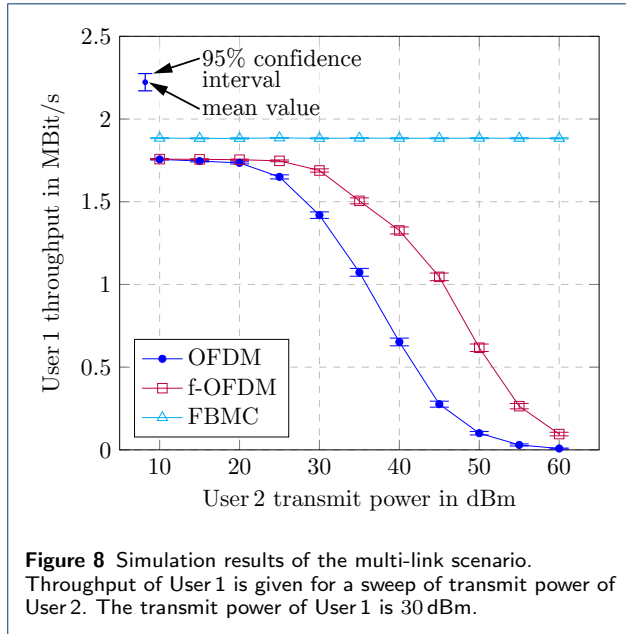
We simulate User 1's throughput for different waveforms, namely OFDM, f-OFDM and FBMC with simulation parameters summarized in Tab. 6. User 1's transmit power is 30 dBm and its path loss is chosen such that it has a high SNR of approximately 40 dB. Results for a sweep over the interfering User 2's transmit power are shown in Fig. 8. We observe that OFDM leads to the highest impact of interference as it has the highest OOB emissions of the three compared waveforms. When OFDM is employed, the throughput of User 1 is already decreasing significantly for a transmit power of 30 dBm of the interfering User 2. For f-OFDM, the impact of interference is also severe, however, due to the filtering and the reduced OOB emissions the drop in throughput occurs only at higher transmit powers of User 2 compared to OFDM. If both users utilize FBMC, then OOB emissions decrease rapidly such that the 60 kHz guard band is sufficient to mitigate IUI. Further, we observe that FBMC leads to a higher spectral efficiency compared to OFDM and f-OFDM as it deploys no CP. The transmit power values of User 2 are swept up to very high values in this simulation. Please note, that this models a situation where the interfering user is close to the BS.

Table 6 Simulation parameters for the multi-link simulation scenario. The effects of IUI are investigated for three different waveforms.

parameter	value		
waveform	OFDM	f-OFDM	FBMC
filter type/length	-	7.14 μ s	PHYDYAS-OQAM
CP length	4.76 μ s	4.76 μ s	-
subcarrier spacing	User 1: 15 kHz, User 2: 30 kHz		
guard band	$2 \times 15 \text{ kHz} + 1 \times 30 \text{ kHz} = 60 \text{ kHz}$		
bandwidth per user	$34 \times 15 \text{ kHz} = 17 \times 30 \text{ kHz} = 0.51 \text{ MHz}$		
modulation/coding	64 QAM/LDPC, $r = 0.65$ (CQI 12)		
channel model	block fading Pedestrian A		

4.8 Non-Orthogonal Multiple Access

Massive connectivity and low latency operation are one of the main drivers for future communications systems. One promising solution addressing these requirements is NOMA [14]. It allows multiple users to share the same orthogonal resources in a non-orthogonal manner. This increases the number of concurrent users and allows them to transmit more often. Currently, the simulator supports a downlink version based on the 3GPP multi-user superposition transmission (MUST) item [70], with more schemes planned for future releases of the simulator. MUST allows the BS to transmit to two users using the same frequency, time, and space by superimposing them in the power-domain. One of those users has good channel conditions (Nearuser), while the other one has bad channel conditions (Faruser), such as a cell-edge user. The



standard defines three power-ratios that control how much power is allocated to each user. In either case, the Faruser gets most of the power in order to help it overcome its harsh conditions. At the receiver side, the interference from the high power user is mitigated by means of successive interference cancellation, or by directly applying ML detection on the superimposed composite constellation.

The remainder of this section is dedicated to an example scenario, introducing the concept of NOMA support within our simulator. In order to demonstrate the gain provided by the 3GPP MUST scheme, we set up the following scenario: two cells, one operating with orthogonal multiple access (OMA), and the other one with NOMA based on MUST. In each cell, the BS splits the bandwidth equally across two strong users; however, since the second BS supports MUST, it can superimpose those two strong users with additional two weak (cell-edge) users, thus providing a cell overloading of 200%. Fig. 9 illustrates the scheduling of the users in the two cells. Notice how the two additional users in the NOMA case occupy the same resources as the main ones, but have a much higher allocated power. The notion of strong and weak users is achieved by choosing an appropriate path-loss for each user's link. Tab. 7 summarizes the simulation parameters for this scenario.

In Fig. 10, the downlink sum-throughput for both the OMA and NOMA cells versus the transmit power of the BSs is plotted. When the transmit power of the BS is low, we observe that MUST is not beneficial, as the interference between the superimposed users has a substantial impact on the performance. However, once

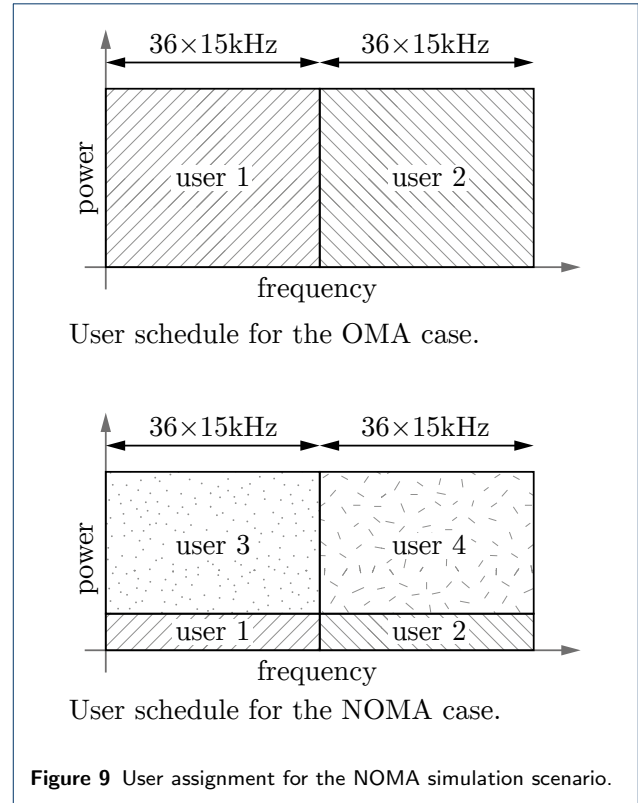
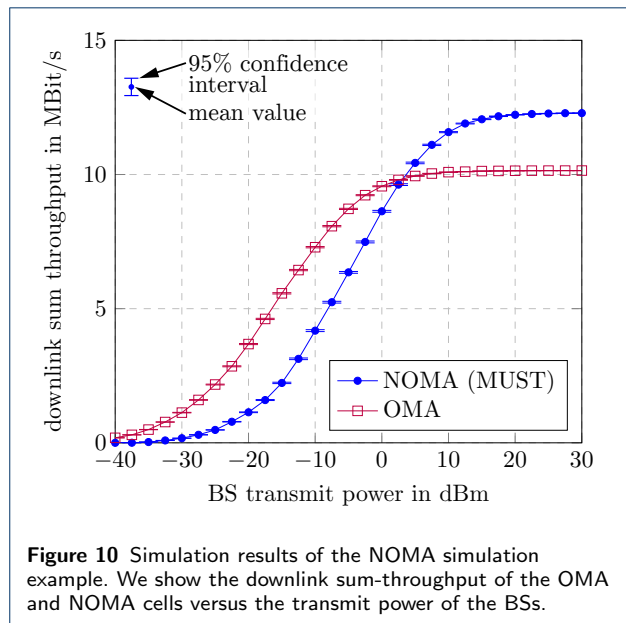


Table 7 The simulation parameters for the NOMA example scenario.

parameter	value	
cells	OMA	NOMA
number of users	2	4 (2 strong, 2 cell-edge)
path-loss	80, 90 dB	strong: 80, 90 dB cell-edge: 110, 115 dB
NOMA receiver	-	ML
MUST power-ratio	-	fixed (second ratio)
bandwidth	1.4 MHz (72 subcarriers)	
waveform/coding	OFDM, LDPC	
MIMO mode	2x2 CLSM	
modulation/code rate	adaptive (CQI based)	
feedback delay	no delay (ideal)	
channel model	Pedestrian A	

the transmit power is sufficiently high, the receiver can carry out the interference suppression more effectively, leading to a considerable gain in the throughput. An improvement of approximately 20% is observed at the transmit power of 15 dBm. This corresponds to the SNRs of 51.6 dB and 41.6 dB for the strong users, and 21.6 dB and 16.6 dB for the weak ones. The SNR here is with respect to the total superimposed received signal. We conclude that, in general, MUST allows the BS to support more users in the downlink, and this, combined with a sufficiently high transmit power, leads to an improved spectral efficiency.



5 Conclusion

For the evolution of mobile communications from LTE to 5G and beyond, an LL simulation is an important tool, enabling research and development of advanced PHY methods. In this contribution, we introduce the Vienna 5G LL Simulator, which is freely available for researchers to support research and enhance reproducibility. We give a general overview of the Vienna 5G LL Simulator, while further supporting documents and details are available at [2]. Further, to outline the overall functionality, examples for specific features are provided, which are included in the simulators download package for increased reproducibility. Our simulator supports standard compliant simulation scenarios and parameter settings, according to current communication specifications such as LTE or 5G NR. Further, versatile functionality in terms of PHY procedures and methods also allows simulation and investigation of potential candidate PHY schemes beyond 5G. The flexible and modular implementation additionally allows for easy augmentation of the simulator, e.g., implementation of additional features, making it a valuable tool for mobile communications research.

Acknowledgements

This work has been funded by the Christian Doppler Laboratory for Dependable Wireless Connectivity for the Society in Motion. The financial support by the Austrian Federal Ministry of Science, Research and Economy and the National Foundation for Research, Technology and Development is gratefully acknowledged.

Author details

¹Christian Doppler Laboratory for Dependable Wireless Connectivity for the Society in Motion. ²Institute of Telecommunications, TU Wien, Gußhausstraße 25/389, 1040 Vienna, Austria.

References

- Mehlführer, C., Ikuno, J.C., Simko, M., Schwarz, S., Rupp, M.: The Vienna LTE simulators — Enabling Reproducibility in Wireless Communications Research. *EURASIP Journal on Advances in Signal Processing (JASP) special issue on Reproducible Research* **2011**(1), 1–14 (2011)
- Institute of Telecommunications, TU Wien: Vienna Cellular Communications Simulators. www.tc.tuwien.ac.at/vccs/ Accessed 12 April 2018
- Rupp, M., Schwarz, S., Taranetz, M.: *The Vienna LTE-Advanced Simulators: Up and Downlink, Link and System Level Simulation*, 1st edn. Signals and Communication Technology. Springer, Singapore (2016). doi:10.1007/978-981-10-0617-3
- Ikuno, J.C., Wrulich, M., Rupp, M.: System level simulation of LTE networks. In: *IEEE Vehicular Technology Conference (VTC Spring)*, Taipei, Taiwan (2010). IEEE
- Taranetz, M., Blazek, T., Kropfreiter, T., Müller, M.K., Schwarz, S., Rupp, M.: Runtime precoding: Enabling multipoint transmission in LTE-advanced system level simulations. *IEEE Access* **3**, 725–736 (2015)
- Zöchmann, E., Schwarz, S., Pratschner, S., Nagel, L., Lerch, M., Rupp, M.: Exploring the physical layer frontiers of cellular uplink. *EURASIP Journal on Wireless Communications and Networking* **2016**(1), 1–18 (2016). doi:10.1186/s13638-016-0609-1
- Schwarz, S., Ikuno, J.C., Simko, M., Taranetz, M., Wang, Q., Rupp, M.: Pushing the limits of LTE: A survey on research enhancing the standard. *IEEE Access* **1**, 51–62 (2013). doi:10.1109/ACCESS.2013.2260371
- Lu, L., Li, G.Y., Swindlehurst, A.L., Ashikhmin, A., Zhang, R.: An overview of massive MIMO: Benefits and challenges. *IEEE Journal of Selected Topics in Signal Processing* **8**(5), 742–758 (2014)
- Larsson, E., Edfors, O., Tufvesson, F., Marzetta, T.: Massive MIMO for next generation wireless systems. *IEEE Communications Magazine* **52**(2), 186–195 (2014)
- Ji, H., Kim, Y., Lee, J., Onggosanusi, E., Nam, Y., Zhang, J., Lee, B., Shim, B.: Overview of full-dimension MIMO in LTE-Advanced pro. *IEEE Communications Magazine* **55**(2), 176–184 (2017)
- Zaidi, A.A., Baldemair, R., Tullberg, H., Björkegren, H., Sundstrom, L., Medbo, J., Kilinc, C., Silva, I.D.: Waveform and numerology to support 5G services and requirements. *IEEE Communications Magazine* **54**(11), 90–98 (2016)
- Guan, P., Wu, D., Tian, T., Zhou, J., Zhang, X., Gu, L., Benjebbour, A., Iwabuchi, M., Kishiyama, Y.: 5G field trials: OFDM-based waveforms and mixed numerologies. *IEEE Journal on Selected Areas in Communications* **35**(6), 1234–1243 (2017)
- Ali, K.S., Elsayy, H., Chaaban, A., Alouini, M.S.: Non-orthogonal multiple access for large-scale 5G networks: Interference aware design. *IEEE Access* **5**, 21204–21216 (2017)
- Ding, Z., Lei, X., Karagiannis, G.K., Schober, R., Yuan, J., Bhargava, V.K.: A survey on non-orthogonal multiple access for 5G networks: Research challenges and future trends. *IEEE Journal on Selected Areas in Communications* **35**(10), 2181–2195 (2017)
- Heath, R.W., González-Prelcic, N., Rangan, S., Roh, W., Sayeed, A.M.: An overview of signal processing techniques for millimeter wave MIMO systems. *IEEE Journal of Selected Topics in Signal Processing* **10**(3), 436–453 (2016)
- Roh, W., Seol, J.Y., Park, J., Lee, B., Lee, J., Kim, Y., Cho, J., Cheun, K., Aryanfar, F.: Millimeter-wave beamforming as an enabling technology for 5G cellular communications: theoretical feasibility and prototype results. *IEEE Communications Magazine* **52**(2), 106–113 (2014)
- Schwarz, S., Rupp, M.: Exploring coordinated multipoint beamforming strategies for 5G cellular. *IEEE Access* **2**, 930–946 (2014). doi:10.1109/ACCESS.2014.2353137
- Clerckx, B., Joudé, H., Hao, C., Dai, M., Rassouli, B.: Rate splitting for MIMO wireless networks: A promising PHY-layer strategy for LTE evolution. *IEEE Communications Magazine* **54**(5), 98–105 (2016)
- Zhao, N., Yu, F.R., Jin, M., Yan, Q., Leung, V.C.M.: Interference alignment and its applications: A survey, research issues, and challenges. *IEEE Communications Surveys Tutorials* **18**(3), 1779–1803 (2016)

20. Piro, G., Grieco, L.A., Boggia, G., Capozzi, F., Camarda, P.: Simulating LTE cellular systems: An open-source framework. *IEEE Transactions on Vehicular Technology* **60**(2), 498–513 (2011)
21. Bültmann, D., Mühleisen, M., Klagges, K., Schinnenburg, M.: openWNS - open wireless network simulator. In: *European Wireless Conference*, pp. 205–210 (2009). IEEE
22. Domínguez-Bolaño, T., Rodríguez-Piñeiro, J., García-Naya, J.A., Castedo, L.: The GTEC 5G link-level simulator. In: *International Workshop on Link-and System Level Simulations (IWLSL)*, pp. 1–6 (2016). IEEE
23. Henderson, T.R., Lacage, M., Riley, G.F., Dowell, C., Kopena, J.: Network simulations with the ns-3 simulator. *SIGCOMM demonstration* **14**(14), 527 (2008)
24. Piro, G., Baldo, N., Miozzo, M.: An LTE module for the ns-3 network simulator. In: *Proceedings of the 4th International ICST Conference on Simulation Tools and Techniques*, pp. 415–422 (2011). ICST (Institute for Computer Sciences, Social-Informatics and Telecommunications Engineering)
25. Mezzavilla, M., Dutta, S., Zhang, M., Akdeniz, M.R., Rangan, S.: 5G mmwave module for the ns-3 network simulator. In: *Proceedings of the 18th ACM International Conference on Modeling, Analysis and Simulation of Wireless and Mobile Systems*, pp. 283–290 (2015). ACM
26. Mezzavilla, M., Zhang, M., Polese, M., Ford, R., Dutta, S., Rangan, S., Zorzi, M.: End-to-end simulation of 5G mmWave networks. *arXiv preprint arXiv:1705.02882* (2017)
27. Nikaein, N., Marina, M.K., Manickam, S., Dawson, A., Knopp, R., Bonnet, C.: OpenAirInterface: A flexible platform for 5G research. *ACM SIGCOMM Computer Communication Review* **44**(5), 33–38 (2014)
28. Jaeckel, S., Raschkowski, L., Börner, K., Thiele, L.: QuaDRiGa: A 3-D multi-cell channel model with time evolution for enabling virtual field trials. *IEEE Transactions on Antennas and Propagation* **62**(6), 3242–3256 (2014)
29. Samimi, M.K., Rappaport, T.S.: 3-D millimeter-wave statistical channel model for 5G wireless system design. *IEEE Transactions on Microwave Theory and Techniques* **64**(7), 2207–2225 (2016)
30. Sun, S., MacCartney, G.R., Rappaport, T.S.: A novel millimeter-wave channel simulator and applications for 5G wireless communications. In: *International Conference on Communications (ICC)*, pp. 1–7 (2017). IEEE
31. 3rd Generation Partnership Project (3GPP): Evolved Universal Terrestrial Radio Access (E-UTRA) physical channels and modulation. TS 36.211, 3GPP (January 2015)
32. 3rd Generation Partnership Project (3GPP): Technical Specification Group Radio Access Network; NR; Physical channels and modulation. TS 38.211, 3GPP (December 2017)
33. 3rd Generation Partnership Project (3GPP): Evolved Universal Terrestrial Radio Access (E-UTRA); Multiplexing and channel coding. TS 36.212, 3GPP (December 2017)
34. 3rd Generation Partnership Project (3GPP): Technical Specification Group Radio Access Network; NR; Multiplexing and channel coding. TS 38.212, 3GPP (December 2017)
35. Tahir, B., Rupp, M.: New construction and performance analysis of polar codes over AWGN channels. In: *24th International Conference on Telecommunications (ICT)*, pp. 1–4 (2017). doi:[10.1109/ICT.2017.7998250](https://doi.org/10.1109/ICT.2017.7998250)
36. Bahl, L., Cocke, J., Jelinek, F., Raviv, J.: Optimal decoding of linear codes for minimizing symbol error rate (Corresp.). *IEEE Transactions on Information Theory* **20**(2), 284–287 (1974). doi:[10.1109/TIT.1974.1055186](https://doi.org/10.1109/TIT.1974.1055186)
37. Koch, W., Baier, A.: Optimum and sub-optimum detection of coded data disturbed by time-varying intersymbol interference [applicable to digital mobile radio receivers]. In: *Global Telecommunications Conference (GLOBECOM)*, pp. 1679–16843 (1990). doi:[10.1109/GLOBECOM.1990.116774](https://doi.org/10.1109/GLOBECOM.1990.116774)
38. Cheng, J.-F., Ottosson, T.: Linearly approximated log-MAP algorithms for turbo decoding. In: *51st Vehicular Technology Conference Proceedings*, vol. 3, pp. 2252–22563 (2000). doi:[10.1109/VETECS.2000.851673](https://doi.org/10.1109/VETECS.2000.851673)
39. MacKay, D.J.C.: Good error-correcting codes based on very sparse matrices. *IEEE Transactions on Information Theory* **45**(2), 399–431 (1999). doi:[10.1109/18.748992](https://doi.org/10.1109/18.748992)
40. Chen, J., Dholakia, A., Eleftheriou, E., Fossorier, M.P.C., Hu, X.-Y.: Reduced-complexity decoding of LDPC codes. *IEEE Transactions on Communications* **53**(8), 1288–1299 (2005). doi:[10.1109/TCOMM.2005.852852](https://doi.org/10.1109/TCOMM.2005.852852)
41. Mansour, M.M., Shanbhag, N.R.: High-throughput LDPC decoders. *IEEE Transactions on Very Large Scale Integration (VLSI) Systems* **11**(6), 976–996 (2003). doi:[10.1109/TVLSI.2003.817545](https://doi.org/10.1109/TVLSI.2003.817545)
42. Radosavljevic, P., de Baynast, A., Cavallaro, J.R.: Optimized message passing schedules for LDPC decoding. In: *Conference Record of the Thirty-Ninth Asilomar Conference on Signals, Systems and Computers*, pp. 591–595 (2005). doi:[10.1109/ACSSC.2005.1599818](https://doi.org/10.1109/ACSSC.2005.1599818)
43. Arikan, E.: Channel Polarization: A Method for Constructing Capacity-Achieving Codes for Symmetric Binary-Input Memoryless Channels. *IEEE Transactions on Information Theory* **55**(7), 3051–3073 (2009). doi:[10.1109/TIT.2009.2021379](https://doi.org/10.1109/TIT.2009.2021379)
44. Tal, I., Vardy, A.: List decoding of polar codes. In: *IEEE International Symposium on Information Theory Proceedings*, pp. 1–5 (2011). doi:[10.1109/ISIT.2011.6033904](https://doi.org/10.1109/ISIT.2011.6033904)
45. 3rd Generation Partnership Project (3GPP): Technical Specification Group Radio Access Network; Study on New Radio (NR) access technology. TR 38.912, 3GPP (June 2017)
46. Nissel, R., Schwarz, S., Rupp, M.: Filter bank multicarrier modulation schemes for future mobile communications. *IEEE Journal on Selected Areas in Communications* **35**(8), 1768–1782 (2017)
47. Schaich, F., Wild, T.: Subcarrier spacing—a neglected degree of freedom? In: *16th International Workshop on Signal Processing Advances in Wireless Communications (SPAWC)*, pp. 56–60 (2015). IEEE
48. 3rd Generation Partnership Project (3GPP): Evolved Universal Terrestrial Radio Access (E-UTRA); LTE physical layer; General description. TS 36.201, 3GPP (March 2018)
49. Zayani, R., Medjahdi, Y., Shaiek, H., Roviras, D.: WOLA-OFDM: a potential candidate for asynchronous 5G. In: *IEEE Globecom Workshops (GC Wkshps)*, pp. 1–5 (2016). IEEE
50. Schaich, F., Wild, T.: Waveform contenders for 5G—OFDM vs. FBMC vs. UFMC. In: *6th International Symposium on Communications, Control and Signal Processing (ISCCSP)*, pp. 457–460 (2014). IEEE
51. Vakilian, V., Wild, T., Schaich, F., ten Brink, S., Frigon, J.-F.: Universal-filtered multi-carrier technique for wireless systems beyond LTE. In: *IEEE Globecom Workshops (GC Wkshps)*, pp. 223–228 (2013). IEEE
52. Geng, S., Xiong, X., Cheng, L., Zhao, X., Huang, B.: UFMC system performance analysis for discrete narrow-band private networks. In: *6th International Symposium on Microwave, Antenna, Propagation, and EMC Technologies (MAPE)*, pp. 303–307 (2015). IEEE
53. Venkatesan, S., Valenzuela, R.A.: OFDM for 5G: Cyclic prefix versus zero postfix, and filtering versus windowing. In: *International Conference on Communications (ICC)*, pp. 1–5 (2016). IEEE
54. Abdoli, J., Jia, M., Ma, J.: Filtered OFDM: A new waveform for future wireless systems. In: *16th International Workshop on Signal Processing Advances in Wireless Communications (SPAWC)*, pp. 66–70 (2015). IEEE
55. Nissel, R., Rupp, M., Marsalek, R.: FBMC-OQAM in doubly-selective channels: A new perspective on MMSE equalization. In: *IEEE International Workshop on Signal Processing Advances in Wireless Communications (SPAWC)*, Sapporo, Japan (2017)
56. Marijanović, L., Schwarz, S., Rupp, M.: MMSE equalization for FBMC transmission over doubly-selective channels. In: *International Symposium on Wireless Communication Systems (ISWCS)*, pp. 170–174 (2016). IEEE
57. Nissel, R., Blumenstein, J., Rupp, M.: Block frequency spreading: A method for low-complexity MIMO in FBMC-OQAM. In: *IEEE International Workshop on Signal Processing Advances in Wireless Communications (SPAWC)*, Sapporo, Japan (2017)
58. Schwarz, S., Mehlführer, C., Rupp, M.: Calculation of the spatial preprocessing and link adaption feedback for 3rd Generation Partnership Project (3GPP) UMTS/LTE. In: *6th Conference on Wireless Advanced (WiAD)*, pp. 1–6 (2010). IEEE
59. Schwarz, S., Wrulich, M., Rupp, M.: Mutual information based calculation of the precoding matrix indicator for 3rd Generation Partnership Project (3GPP) UMTS/LTE. In: *International ITG*

- Workshop on Smart Antennas (WSA), pp. 52–58 (2010). IEEE
60. Ademaj, F., Taranetz, M., Rupp, M.: 3GPP 3D MIMO channel model: A holistic implementation guideline for open source simulation tools. *EURASIP Journal on Wireless Communications and Networking* **2016**(1), 55 (2016). doi:[10.1186/s13638-016-0549-9](https://doi.org/10.1186/s13638-016-0549-9)
 61. 3rd Generation Partnership Project (3GPP): Study on 3D channel model for LTE. TR 36.873, 3GPP (June 2015)
 62. 3rd Generation Partnership Project (3GPP): Technical Specification Group Radio Access Network; High Speed Downlink Packet Access: UE Radio Transmission and Reception. TR 25.890, 3GPP (May 2002)
 63. 3rd Generation Partnership Project (3GPP): Technical Specification Group Radio Access Network; Study on channel model for frequencies from 0.5 to 100GHz. TR 38.901, 3GPP (December 2017)
 64. 3rd Generation Partnership Project (3GPP): Technical Specification Group Radio Access Network; Evolved Universal Terrestrial Radio Access: Base Station radio transmission and reception. TR 36.104, 3GPP (December 2017)
 65. Zheng, Y.R., Xiao, C.: Simulation models with correct statistical properties for rayleigh fading channels. *IEEE Transactions on communications* **51**(6), 920–928 (2003)
 66. Zemen, T., Mecklenbräuker, C.F.: Time-variant channel estimation using discrete prolate spheroidal sequences. *IEEE Transactions on signal processing* **53**(9), 3597–3607 (2005)
 67. Durgin, G.D., Rappaport, T.S., Wolf, D.A.D.: New analytical models and probability density functions for fading in wireless communications. *IEEE Transactions on Communications* **50**(6), 1005–1015 (2002)
 68. 3rd Generation Partnership Project (3GPP): Evolved Universal Terrestrial Radio Access (E-UTRA); User Equipment (UE) radio transmission and reception. TS 36.101, 3GPP (December 2017)
 69. Marijanović, L., Schwarz, S., Rupp, M.: Optimal numerology in OFDM systems based on imperfect channel knowledge. In: 87th Vehicular Technology Conference: VTC2018-Spring (2018). IEEE
 70. 3rd Generation Partnership Project (3GPP): Technical Specification Group Radio Access Network; Study on Downlink Multiuser Superposition Transmission (MUST) for LTE. TR 36.859, 3GPP (December 2015)